

LA-UR -81-1511

TITLE: ~~MASTER~~ MULTI-ENERGY GAMMA-RAY AUTOMATED SCANNING SYSTEM

AUTHOR(S): Hsiao-Hua Hsu, Group Q-2
John C. Pratt, Group Q-2
Edward R. Shunk, Group Q-2

SUBMITTED TO: Fifth Symposium on X- and Gamma-Ray
Sources and Applications
Ann Arbor, Michigan
June 10-12, 1981

100% APPROX

University of California

In acceptance of this article, the publisher recognizes that the U.S. Government retains a nonexclusive, royalty-free license to publish or reproduce the published form of the contribution or to allow others to do so, for U.S. Government purposes.

The Los Alamos Scientific Laboratory requests that the publisher identify the article as work performed under the auspices of the U.S. Department of Energy.



LOS ALAMOS SCIENTIFIC LABORATORY

Post Office Box 1663 Los Alamos, New Mexico 87545

An Affirmative Action Equal Opportunity Employer

EXCELSIOR CONSULTING GROUP

DOE LA-UR-81-1511
Rev. 5-29
JULY 1981

UNITED STATES
DEPARTMENT OF ENERGY
CONTRACT DE-AC04-76ER00016

MULTI-ENERGY GAMMA-RAY AUTOMATED SCANNING SYSTEM

H. H. Hsu, J. C. Pratt, and E. R. Shunk

Los Alamos National Laboratory
Los Alamos, New Mexico, 87545, USA

ABSTRACT

A CAMAC-based gamma-ray scanning system was used to measure the transmission through stacked attenuators for up to 16 different gamma rays. For each measurement, we obtained the transmission for gamma rays ranging in energy from 77 to 2614 keV. These transmission measurements were used to produce a set of linear equations that may be solved for either thickness or density of the discrete attenuators comprising a given stacked assembly.

INTRODUCTION

A CAMAC automated scanning system¹ was used for multi-energy transmission measurements. These measurements allowed us to estimate the position of separate thicknesses of stacked discrete attenuators.

EXPERIMENTAL SETUP

The gamma-ray source used in this experiment was an Am^{241} point source located approximately 1 cm from a selected gamma ray detector. A scanner carriage, translatable along the horizontal axis, holds the attenuating stack along the beamline to the detector source axis, as illustrated in Fig. 1. The scanner carriage is positioned by a drive screw turned by a stepper motor that is controlled by the data acquisition system.

A LeCroy 3500 multichannel analyzer was used to acquire and store the data for subsequent analysis. The LeCroy 3500 has a built-in CAMAC minicrate, keyboard, and cathode-ray tube display (Fig. 2). It runs a CP/M[™] operating system that supports FORTRAN programs. LeCroy supplied both a FORTRAN-callable CAMAC program and plotting libraries that were used to develop the data-acquisition software employed in making these measurements.

The LeCroy 3500 also has special CAMAC data acquisition modules that can initiate direct memory access (DMA) to the 24-bit data memory. One such module is the LeCroy 3511 analog-to-digital converter that detects and digitizes the gamma-ray detector pulses. The digitizing time for 13 bits is 5 μ s; the DMA time is 1 μ s. With this module programmed to deliver its data by direct memory access, the gamma spectra acquisition continues without impact on the computation.

We acquired a transmitted gamma-ray spectrum for each horizontal point considered, then controlled the stepping motor to position the carriage to the next point. At the end of the operator-specified acquisition time for each of those points, we read the data memory and calculated the net photopeak area for each of up to 10 separate gamma rays. The ratio of each transmitted gamma ray's count rate to the count rate with the object (or stack of attenuators) removed, is the transmission of the material(s) at that point.

EXPERIMENTAL METHOD

Specific probe monoenergetic gamma rays were chosen as widely separated in energy as possible in order to have a suitably large range of material attenuation coefficients. A ^{238}Th - ^{208}Tl source comes very close to these requirements, decays with a long half-life, and is readily available. On occasion, a ^{60}Co source was incorporated for acquiring better statistics in the middle of the energy range employed.

One gamma-ray transmission scan of a multiple-component/multiple-layer attenuating assembly appears in Fig. 3. The arrangement of the attenuating materials is shown in Fig. 4. The scan shows a series of irregular steps as the scanner transports the attenuator assembly through the gamma-ray beam. The boundaries between materials appear on the plot. The measured transmission occasionally increases markedly at boundary points where poor joints allow a straight-through path for source gamma rays. One such spatial scan was recorded for each gamma ray.

If we denote

$I_0(k)$ = intensity of gamma-ray k without absorber,

$I(k)$ = intensity of gamma-ray k with absorber,

ρ_i = density of absorber i , in g/cm^3 ,

$\mu_i(k)$ = attenuation coefficient of absorber i at the energy of gamma-ray k , in cm^{-1}/g , and

t_i = thickness of absorber i , in cm,

then the transmission ratio $I(k)/I_0(k)$ is given for the materials present by

$$I(k) = I_0(k) \exp -\sum_i \mu_i(k) \rho_i t_i \quad (1a)$$

or

$$\ln \frac{I_0}{I} = \sum_i \mu_i(k) \rho_i t_i. \quad (1b)$$

One such equation, relating the material thicknesses (or densities) to observed gamma-ray intensities, is obtained for each gamma ray.

EXAMPLE

Consider the following seven gamma rays of ^{226}Th - ^{208}Tl , ^{133}Ba , and ^{60}Co : 238, 356, 583, 860, 1332, 1620, and 2614 keV. Imagine these gamma rays impinging upon some composite structure made up of the materials shown in Table I.

If we take the densities and attenuation coefficients as known, the thickness of each material remains unknown on the right-hand side of equation (1b), which when expanded produces the following set of seven equations in six unknowns:

$$\frac{I_0}{I(238)} = 7.08 t_1 + 1.90 t_2 + 0.946 t_3 + 0.403 t_4 + 0.121 t_5 + 0.718 t_6 \quad (2a)$$

$$\frac{I_0}{I(356)} = 0.10 t_1 + 1.10 t_2 + 0.371 t_3 + 0.261 t_4 + 0.105 t_5 + 0.188 t_6 \quad (2b)$$

$$\frac{I_0}{I(583)} = 1.01 t_1 + 0.761 t_2 + 0.699 t_3 + 0.210 t_4 + 0.061 t_5 + 0.156 t_6 \quad (2c)$$

$$\frac{I_0}{I(860)} = 0.890 t_1 + 0.547 t_2 + 0.496 t_3 + 0.178 t_4 + 0.036 t_5 + 0.128 t_6 \quad (2d)$$

$$\frac{I_0}{I(1332)} = 0.015 t_1 + 0.029 t_2 + 0.020 t_3 + 0.006 t_4 + 0.001 t_5 + 0.006 t_6 \quad (2e)$$

$$\frac{I_0}{I(1620)} = 0.011 t_1 + 0.009 t_2 + 0.009 t_3 + 0.001 t_4 + 0.001 t_5 + 0.008 t_6 \quad (2f)$$

$$\frac{I_0}{I(2614)} = 0.007 t_1 + 0.007 t_2 + 0.007 t_3 + 0.001 t_4 + 0.000 t_5 + 0.007 t_6 \quad (2g)$$

where t_1 , t_2 , t_3 , t_4 , t_5 , t_6 are the thicknesses (in centimeters) of lead, cadmium, iron, aluminum, polyethylene, and mock high explosive, respectively. One such set of linear equations occurs at each point in a typical scan, relating the thicknesses of the materials at that point to the transmission of the gamma rays at that point.

We can find these unknown thicknesses $t_1 \dots t_6$ by solving the set of six linear equations exactly, or finding the t_i by a least-squares method where there are more equations than unknowns. The results of a test run appear in Table II.

Inferred attenuator thickness values were, in general, lower than the actual thickness for each specific attenuating material. The observed difference can be attributed to the fact that the employed theoretical attenuation coefficients for these materials were derived from narrow beam considerations, an ideal situation not too well realized in the actual measurements.

REFERENCE

1. C. E. New, J. C. Pratt, and F. R. Shunk, "A CAMAC Gamma-Ray Scanning System," Fifth Symposium on X- and Gamma-Ray Sources and Applications, Ann Arbor, Michigan, June 10-12, 1981.

TABLE I
LINEAR ATTENUATION COEFFICIENTS AT VARIOUS GAMMA ENERGIES

Gamma-ray energy (keV)	Material					
	Lead $\rho=11.3$ (cm^{-1})	Cadmium $\rho=0.65$ (cm^{-1})	Iron $\rho=7.86$ (cm^{-1})	Aluminum $\rho=2.70$ (cm^{-1})	Polyethylene $\rho=0.92$ (cm^{-1})	Nock High Explosive $\rho=1.84$ (cm^{-1})
160.0	7.076	1.90	0.959	0.303	0.121	0.218
311.0	4.25	1.35	0.831	0.278	0.112	0.200
550.0	3.10	1.10	0.765	0.261	0.105	0.188
911.7	1.70	0.776	0.647	0.225	0.0907	0.163
5e3.2	1.41	0.701	0.609	0.216	0.0857	0.154
727.3	1.17	0.604	0.549	0.193	0.0777	0.139
1173.2	0.897	0.545	0.506	0.178	0.0719	0.128
1831.3	0.660	0.458	0.433	0.153	0.0618	0.111
2629.8	0.528	0.429	0.407	0.144	0.0579	0.104
3614.7	0.476	0.390	0.369	0.130	0.0523	0.0938
4614.7	0.476	0.327	0.300	0.120	0.0403	0.0726

TABLE II

ACTUAL AND EXPERIMENTAL ATTENUATOR THICKNESSES

	<u>Lead (cm)</u>	<u>Cadmium (cm)</u>	<u>Iron (cm)</u>	<u>Aluminum (cm)</u>	<u>Polyethylene (cm)</u>	<u>Mock High Explosive (cm)</u>
Actual	1.9	0.32	2.5	1.9	5.4	6.6
Measured	1.9 ± 0.3	0.28 ± 0.3	2.3 ± 0.3	1.7 ± 0.3	5.0 ± 0.5	5.9 ± 0.7

FIGURE CAPTIONS

Fig. 1. High-purity germanium detector, source, and attenuation materials mounted on scanner carriage.

Fig. 2. LeCroy 3500 multichannel analyzer.

Fig. 3. Attenuation profile, multi-component/multi-layer transmission test object.

Fig. 4. Top view of transmission test object shown in Fig. 3.

$$\ln \frac{i_0(235)}{i(235)} = 7.08 t_1 + 1.90 t_2 + 0.959 t_3 + 0.303 t_4 + 0.121 t_5 + 0.218 t_6 \quad (2a)$$

$$\ln \frac{i_0(355)}{i(355)} = 3.10 t_1 + 1.10 t_2 + 0.765 t_3 + 0.261 t_4 + 0.105 t_5 + 0.188 t_6 \quad (2b)$$

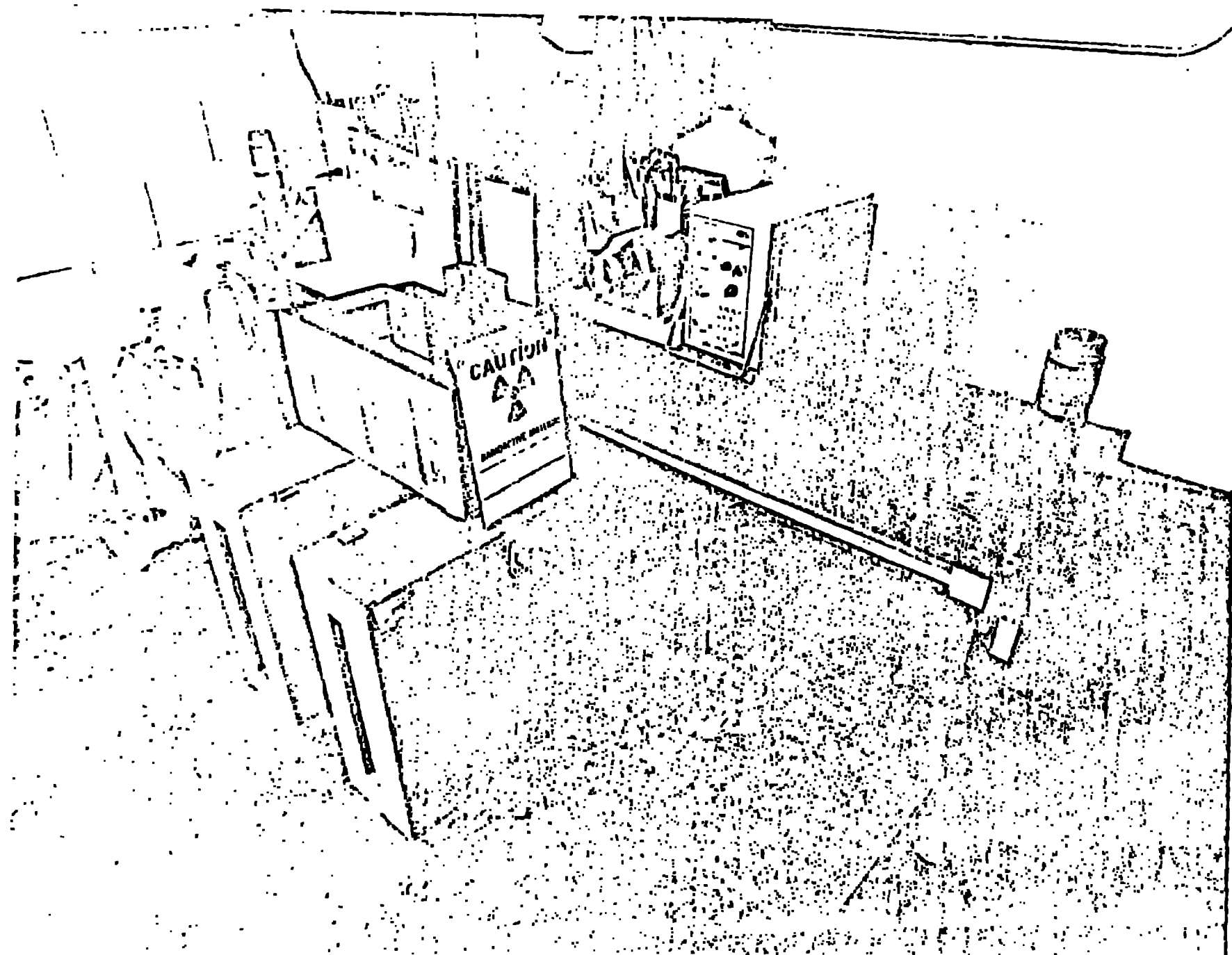
$$\ln \frac{i_0(563)}{i(563)} = 1.41 t_1 + 0.701 t_2 + 0.609 t_3 + 0.216 t_4 + 0.085 t_5 + 0.154 t_6 \quad (2c)$$

$$\ln \frac{i_0(860)}{i(860)} = 0.697 t_1 + 0.545 t_2 + 0.506 t_3 + 0.178 t_4 + 0.0719 t_5 + 0.128 t_6 \quad (2d)$$

$$\ln \frac{i_0(1332)}{i(1332)} = 0.526 t_1 + 0.429 t_2 + 0.407 t_3 + 0.144 t_4 + 0.0579 t_5 + 0.104 t_6 \quad (2e)$$

$$\ln \frac{i_0(1620)}{i(1620)} = 0.561 t_1 + 0.390 t_2 + 0.369 t_3 + 0.130 t_4 + 0.0523 t_5 + 0.0938 t_6 \quad (2f)$$

$$\ln \frac{i_0(2614)}{i(2614)} = 0.476 t_1 + 0.327 t_2 + 0.300 t_3 + 0.102 t_4 + 0.0403 t_5 + 0.0726 t_6 \quad (2g)$$



LeCroy 3500

